Ther Adv Neurol Disord

2019, Vol. 12: 1–16

DOI: 10.1177/1756286419877081

2D *in-vivo* L-COSY spectroscopy identifies neurometabolite alterations in treated multiple sclerosis

Scott Quadrelli, Karen Ribbons, Jameen Arm, Oun Al-iedani, Jeannette Lechner-Scott, Rodney Lea and Saadallah Ramadan

Abstract

Background: We have applied *in vivo* two-dimensional (2D) localized correlation spectroscopy (2D L-COSY), in treated relapsing relapsing-remitting multiple sclerosis (RRMS) to identify novel biomarkers in normal-appearing brain parenchyma.

Methods: 2D L-COSY magnetic resonance spectroscopy (MRS) spectra were prospectively acquired from the posterior cingulate cortex (PCC) in 45 stable RRMS patients undergoing treatment with Fingolimod, and 40 age and sex-matched healthy control (HC) participants. Average metabolite ratios and clinical symptoms including, disability, cognition, fatigue, and mental health parameters were measured, and compared using parametric and nonparametric tests. Whole brain volume and MRS voxel morphometry were evaluated using SIENAX and the SPM LST toolbox.

Results: Despite the mean whole brain lesion volume being low in this RRMS group (6.8 ml) a significant reduction in PCC metabolite to tCr ratios were identified for multiple N-acetylaspartate (NAA) signatures, gamma-aminobutyric acid (GABA), glutamine and glutamate (Glx), threonine, and isoleucine/lipid. Of the clinical symptoms measured, visuospatial function, attention, and memory were correlated with NAA signatures, Glx, and isoleucine/lipid in the brain.

Conclusions: 2D L-COSY has the potential to detect metabolic alterations in the normal-appearing MS brain. Despite examining only a localised region, we could detect metabolic variability associated with symptoms.

Keywords: 2D L-COSY, RRMS, Multiple Sclerosis, Magnetic Resonance, Spectroscopy, MRS

Received: 20 November 2018; revised manuscript accepted: 15 August 2019.

Correspondence to:
Jeannette Lechner-Scott
Department of Neurology, John Hunter Hospital, Newcastle, NSW, Australia
Jeannette.LechnerScott@health.nsw.gov.au

Hunter Medical Research Institute, Newcastle, NSW, Australia

School of Medicine and Public Health, Faculty of Health and Medicine, University of Newcastle, Callaghan, NSW, Australia

Scott Quadrelli
Institute of Health and Biomedical Innovation, Queensland University of Technology, Brisbane, QLD, Australia

School of Health Sciences, Faculty of Health and Medicine, University of Newcastle, Callaghan, NSW, Australia

Department of Radiology, Princess Alexandra Hospital, Brisbane, QLD, Australia

Faculty of Medicine, University of Queensland, Brisbane, QLD, Australia

Karen Ribbons
Department of Neurology, John Hunter Hospital, Newcastle, NSW, Australia

Jameen Arm
School of Health Sciences, Faculty of Health and Medicine, University of Newcastle, Callaghan, NSW, Australia

Radiological Imaging Services, Hunter New England Local Health District, NSW, Australia

Oun Al-iedani
Saadallah Ramadan
School of Health Sciences, Faculty of Health and Medicine, University of Newcastle, Callaghan, NSW, Australia

Introduction

Multiple Sclerosis (MS) is a chronic immune-mediated demyelinating condition. Disease severity is monitored using clinical symptoms and magnetic resonance imaging (MRI) of the brain. In recently published guidelines for the management of MS cases, brain and spinal cord MRI play a prominent role in the diagnosis and follow up of dissemination in time and space of central nervous system (CNS) involvement.[1] There is increased reliance on MRI in the clinical management of MS, however, as a primary outcome measure in therapeutic trials, MRI biomarkers are limited. There is a clinico-radiological paradox, such that there can be a poor association between clinical findings and radiological disease severity.[1–3] Next to multifocal white matter lesions, other contributing pathological features remain unrecognized due to the limitation of conventional MRI protocols (such as T1 and T2 weighted imaging) to detect CNS changes, including functional alterations in normal appearing brain matter (NABM). Changes in NABM, grey matter lesions,[4] and neurodegeneration, lead eventually to brain atrophy and accumulating disability during the course of the disease.[5,6] In addition, following the sharp

Rodney Lea
Institute of Health and Biomedical Innovation, Queensland University of Technology, Brisbane, QLD, Australia
Hunter Medical Research Institute, Newcastle, NSW, Australia

increase in the number of new disease modifying therapies available for the treatment of MS in the last decade, it has become essential to better understand the underlying pathological changes associated with disease progression and thereby develop new meaningful imaging biomarkers to radiologically evaluate the clinical efficacy of treatments.

Total brain volume and atrophy have been correlated with overall disability status,[7] while grey matter volume[6,8] has a strong predictive value with both physical disability and cognitive impairment in MS. Other novel MRI metrics enable metabolic changes in the MS brain to be explored, and have the potential to provide biomarkers of disease progression. Proton magnetic resonance spectroscopy imaging (H^1-MRS) is a noninvasive technique allowing an evaluation of cerebral metabolites altering functional processes in the MS brain.[9,10] Studies conducted to date have been able to demonstrate metabolic changes occurring across multiple regions in the MS brain, and that these alterations are not restricted to active white matter lesions, but also occur in regions of NABM.[11] By far the most common metabolite evaluated by MRS in MS has been N-acetylaspartate (NAA), with reduction in NAA associated with axonal loss, neuronal damage, and mitochondrial dysfunction.[12] Levels of NAA have been correlated with disability status and disease course, [13–15] with the magnitude of change differing between brain regions as well as between lesions and NABM.[4,11] NAA levels have also been associated with the efficacy of MS therapies.[13,16]

Conventional H^1-MRS is limited by the number of metabolites that can be quantified, due to overlapping resonances from the neurotransmitters such as glutamate, glutamine, and gamma-aminobutyric acid (GABA), making evaluation of their potential role in MS difficult. For example, GABA has been proposed as a marker of neurodegeneration; however, it cannot be reliably quantified by conventional MRS.[17] An alternative approach is two-dimensional (2D) MRS, which compensates for the limitations of conventional MRS, as it allows composite or overlapping resonances from 1D spectra to be separated out. In conventional 1D spectroscopy, intensity (y-axis) is plotted against frequency (x-axis), whereas, in 2D spectroscopy, the intensity is plotted against two frequency variables.[18] The introduction of 2D *in vivo* spectroscopy has allowed researchers to make unambiguous metabolite assignments, that previously could not have been made using 1D spectroscopy,[19–21] with 2D localized correlation spectroscopy (2D L-COSY) being shown as a reliable method for *in vivo* detection of brain metabolites.[22]

We hypothesized that 2D spectroscopy would yield additional metabolic information in MS, not available using conventional MRS. The aim of the current work was to identify neurochemical differences in the NABM of clinically stable relapsing remitting MS (RRMS) patients all treated with the same immunotherapy, compared with age and sex-matched healthy individuals, using 2D L-COSY. We went on to determine if any of the metabolites identified were associated with clinical symptoms, including disability status, cognitive function, mood status, and fatigue. We also compared associations between features derived from other MRI approaches, including brain volume estimates and lesion load with clinical outcomes, thereby evaluating the benefits of obtaining additional information regarding alterations in metabolic species in the MS brain by 2D L-COSY.

Methods

Subjects

Patients were recruited prospectively from the MS outpatient clinic at John Hunter Hospital, Newcastle, Australia, from December 2014 to June 2017. A total of 45 RRMS patients and 40 age- and sex-matched healthy controls (HC) were studied. Participants were considered age-matched if they were within ± 2 years of age to patients, with age at the time of scanning calculated according to date of birth. Patients were eligible if they had a confirmed diagnosis of RRMS, were aged between 18 and 65 years, had an Expanded Disability Status Scale (EDSS) score from 1 to 4 (able to walk a minimum of 500 m) and were currently undergoing immunomodulatory therapy with Fingolimod. Patients were excluded if they had a comorbid diagnosis of other neurological or psychiatric condition, impaired capacity to consent, any contraindication to MRI scanning, or treatment with glucocorticoids within the last 3 months. HC were recruited from the Hunter Medical Research Institute (HMRI) research registry, and were included if they were aged between 18 and 65 years and had no prior history of neurological

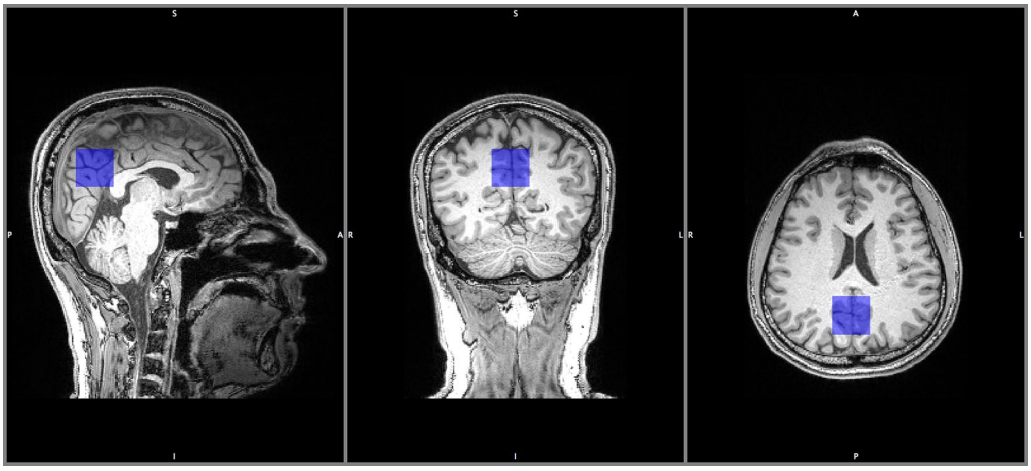

Figure 1. Representative MRS voxel location in the PCC, in a HC participant.
HC, healthy control; MRS, magnetic resonance spectroscopy; PCC, posterior cingulate cortex.

or psychiatric disease. Participants were excluded if they had impaired capacity to consent; any contraindication to MRI scanning; or were receiving opiates, antipsychotics, or benzodiazepines. Demographic data and clinical histories were obtained at the time of study enrolment. Written informed consent was obtained from all participants prior to study commencement and the research protocol was approved by the Hunter New England Local Health District human research ethics committee.

Clinical assessments

MS patients were examined by a neurologist, and their disability status was evaluated using EDSS.[23] All EDSS evaluations were undertaken by a neurologist who had appropriate Neurostatus certification training. EDSS is performed only in MS patients and ranges from 0 to 10, higher values indicate greater disability. The Multiple Sclerosis Severity Score (MSSS) was calculated from the EDSS and duration of disease for each patient using the algorithms provided by Roxburgh and colleagues.[24] Participants were also assessed using the Audio Recorded Cognitive Screen (ARCS), Symbol Digit Modalities Test (SDMT), Depression Anxiety Stress Scales (DASS-21), and Modified Fatigue Impact Scale (MFIS), which are detailed in full in Appendix 1.

MRI protocol

All scans were performed on a 3T Prisma (Siemens, Erlangen, Germany, software version VE11C) with a 64-channel head and neck coil (Siemens, Erlangen, Germany).

Structural imaging. All participants underwent structural imaging that included: three-dimensional (3D) T1-weighted magnetization-prepared rapid gradient echo (MPRAGE) sequence (TR/TE/TI = 2000/3.5/1100 ms, flip angle = 7°, field of view = 256 × 256 mm, voxel size $1 \times 1 \times 1\,mm^3$, IPAT = 2, acquisition time 4:48 min); and T2 fluid attenuated inversion recovery (FLAIR) (TR/TE/TI = 5000/386/1800 ms, echo train duration = 858 ms, field of view = $256 \times 256\,mm^2$, with spatial resolution of $1 \times 1 \times 1\,mm^3$, IPAT = 3, acquisition time 4:12 min).

2D L-COSY MR spectroscopy. A 3D T1 MPRAGE was reconstructed in the sagittal and coronal planes with 2 mm slice resolution for accurate localization of the voxel. NABM in the posterior cingulate cortex (PCC), composed of white and grey matter, was chosen for examination as shown in Figure 1. The PCC was chosen as it is a highly connected and metabolically active brain region,[25] involved in learning and memory,[19] has a favorable location for magnetic field shimming, and is relatively insensitive to motion during spectral acquisition. All data were acquired in the morning to avoid any possible diurnal effects.[26] 2D L-COSY was acquired using 96 increments and eight averages per increment, full acquisition parameters are described in Appendix 1.

2D L-COSY quantification. All participants had satisfactory quality data for analysis. Raw 2D L-COSY

data were transferred to MATLAB (2015b) for signal combination from multiple elements followed by row concatenation into a 2D matrix.[27] Felix, a commercial 2D spectral processing software,[28] was used for spectral processing and analysis. The total creatine (tCr) methyl diagonal resonance, at 3.02 ppm, was used as an internal chemical shift reference in F1 and F2. Our group has performed absolute quantification of tCr separately using 1D spectroscopy, which was found to be stable in NABM in RRMS, confirming that tCr (F2: 3.02–F1: 3.02 ppm) was an appropriate L-COSY internal reference in RRMS. As relative quantification has been utilized as part of this investigation, partial volume correction was not required. All 'cross' or off-diagonal peaks were denoted with (F2–F1) in ppm units. Several species with multiple cross peaks, such as glutamine and glutamate (Glx), NAA and lipid, were also summed together and compared.

Whole brain volume and white matter lesion quantification. FLAIR hyperintensities were segmented using the lesion growth algorithm[29] as implemented in the LST toolbox version 2.0.6 (www.statistical-modelling.de/lst.html) for SPM. See Appendix 1 for full details.

Brain tissue volume, normalized for subject head size, was estimated with SIENAX,[30] part of FSL.[31] See the methods used by SIENAX in Appendix 1.

Statistical analyses

Differences between group means for clinical data, 2D metabolites and neuroimaging metrics were determined using independent-samples *t* tests for means. Bivariate correlations among quantitative test variables were performed using Pearson's *r* tests. Since some of the variables tested deviated from parametric assumptions, we also performed nonparametric equivalent tests for mean differences and bivariate correlation that is, Mann–Whitney *U* test and Spearman's rho tests, respectively. Nonparametric equivalence tests were performed as a partial guard against false positives, and to assist in the interpretation of the parametric test results. Nonparametric and parametric equivalence tests were run across all measures regardless of normality testing. The Bonferroni critical value for group comparison of 2D L-COSY metabolites was calculated to be 0.007. The Bonferroni critical value for Spearman's and Pearson's tests was 0.0000031. However, due to the exploratory nature of this study, we took a *p*-value threshold of 0.05 to be suggestive and the calculated Bonferroni value to be a conclusive threshold.

Results

Participant demographics and characteristics

The RRMS patient cohort was predominantly female (73%), with an average age of 43.4 years. Average disability status was mild (mean EDSS = 2), with an average disease duration of 8 years. Only patients who had been undergoing treatment with the disease modifying therapy Fingolimod for at least 6 months were included in the study. The average treatment duration for the patient cohort at the time of study assessments was 2 years (Table 1). The patient cohort had poorer performance on both the ARCS and SDMT cognitive assessment tasks compared with age and sex-matched HCs. The overall ARCS score, fluency, and visuospatial domain scores were lower in the MS cohort, together with processing speed and attention, as measured by the SDMT. Self-reported ability to perform routine tasks (FAQ) was also worse in MS patients compared with HCs. Mood symptoms were also more pronounced in the MS cohort, with 2-fold higher levels of depression and anxiety and 1.7-fold higher scores for stress compared with the HC group. The MS cohort also reported higher levels of fatigue (p-value $\leqslant 0.001$) than HCs with physical and cognitive fatigue scores increased by 3- and 2-fold (p-value $\leqslant 0.001$ for both indices), respectively.

2D L-COSY

A typical 2D L-COSY spectrum for a HC volunteer and an RRMS participant is shown in Figures 2 and 3 respectively. A summary of the statistically significant neurochemical differences is shown in Table 2. A statistically significant reduction in metabolite to tCr ratios was identified for multiple NAA signatures (labelled NAA-I, NAA-III, and NAA-IV), N-acetylaspartylglutamate (NAAG), Glx, GABA, threonine, and isoleucine/lipid. Additionally, there was a significant reduction in the ratios of summed cross peaks for NAA and Glx. Only the NAA signatures (NAA, NAA-1, total NAA) retained significance after adjusting

Table 1. Participant demographic and clinical features.

	HC	RRMS	*p*-value
n	40	45	–
Age (years)	42.7 ± 1.4	43.4 ± 1.4	0.71
Female (%)	63	73	–
Disease Duration (years)	N/A	7.9 ± 0.9	–
EDSS	N/A	2.0 ± 0.2	–
MSSS	N/A	3.1 ± 0.3	–
Memory	94.8 ± 2.3	88.0 ± 3.7	0.14
Fluency	96.0 ± 2.9	84.7 ± 2.7	0.005*
Visuospatial	102.8 ± 0.6	99.8 ± 0.7	0.01*
Language	91.3 ± 4.2	87.5 ± 3.3	0.5
Attention	99.8 ± 2.5	94.3 ± 2.0	0.07
Total ARCS	94.6 ± 2.7	86.8 ± 2.8	0.05*
SDMT	59.1 ± 1.9	50.9 ± 1.6	0.00*
FAQ	0.7 ± 0.3	3.7 ± 0.9	0.004*
Depression	3.2 ± 0.7	7.5 ± 1.4	0.008*
Anxiety	3.1 ± 0.8	6.7 ± 1.2	0.013*
Stress	7.7 ± 1.2	13.0 ± 1.5	0.01*
Total DASS	14.1 ± 2.4	26.4 ± 3.4	0.005*
Physical Fatigue	5.8 ± 0.9	18.0 ± 1.4	<0.001*
Cognitive Fatigue	7.7 ± 1.1	16.3 ± 1.4	<0.001*
Total Fatigue	13.5 ± 1.8	34.4 ± 2.7	<0.001*

ARCS, Audio Recorded Cognitive Screen; DASS, Depression Anxiety and Stress Scale; EDSS, Expanded Disability Severity Scale; FAQ, Functional Assessment Questionnaire; HC, healthy control; MSSS, Multiple Sclerosis Severity Scale; RRMS, relapsing-remitting multiple sclerosis; SDMT, Symbol Digit Modalities Test.
All data are expressed as mean ± standard error of the mean unless otherwise indicated.
*Indicates significance (p-value ⩽ 0.05) using Mann–Whitney U tests.

for multiple comparisons. Summed lipids were increased (18%) in the RMMS group when compared with HCs, trending towards statistical significance (p-value = 0.054).

No significant difference was identified in the choline-containing compounds, lactate, glutathione, macromolecules, or myo-inositol.

Whole brain and voxel characteristics

The single spectroscopy voxel (SVS) was comprised of 37% white matter (WM), 51% grey matter (GM), and 13% cerebrospinal fluid (CSF). There was no significant difference in the partial volume fractions within the SVS voxel between the RRMS and control groups, as shown in Table 3.

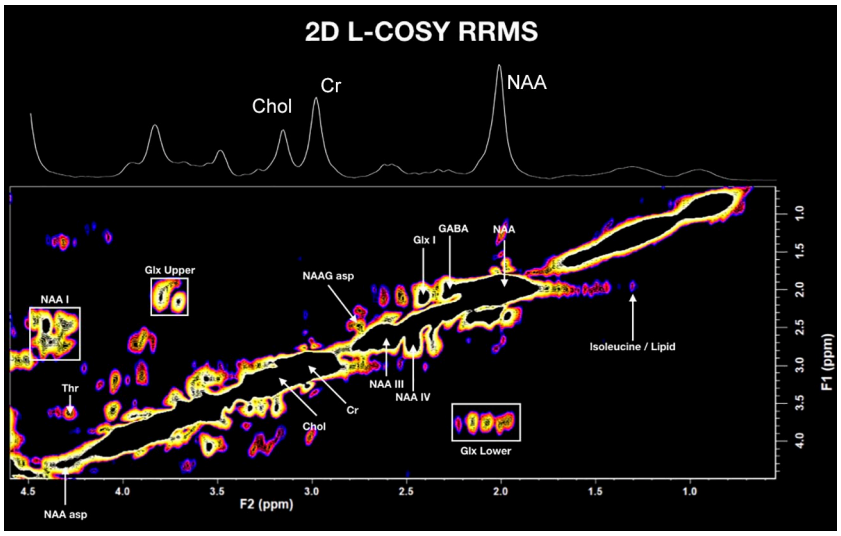

Figure 2. *In vivo* L-COSY of a patient with RRMS (PCC) acquired at 3T, using a 64 channel head and neck coil; voxel size $30 \times 30 \times 30\,mm^3$, increment size 0.8 ms, increments 96, 8 averages per increment, TR 1.5 sec, total experimental time 19 min, acquired vector: 1024 points, acquisition time: 512 ms, spectral width in F2: 2000 Hz, spectral width F1: 1250 Hz.
Cr, Creatine; Chol, Choline; GABA, gamma-aminobutyric acid; Glx, glutamine and glutamate cross peaks; L-COSY, localized correlation spectroscopy; PCC, posterior cingulate cortex; NAA, N-acetylaspartate; NAA-I, III and IV, additional N-acetylaspartate signatures; NAA asp, NAA aspartate moiety; NAAG, N-acetylaspartylglutamate; RRMS, relapsing-remitting multiple sclerosis; Thr, Threonine.

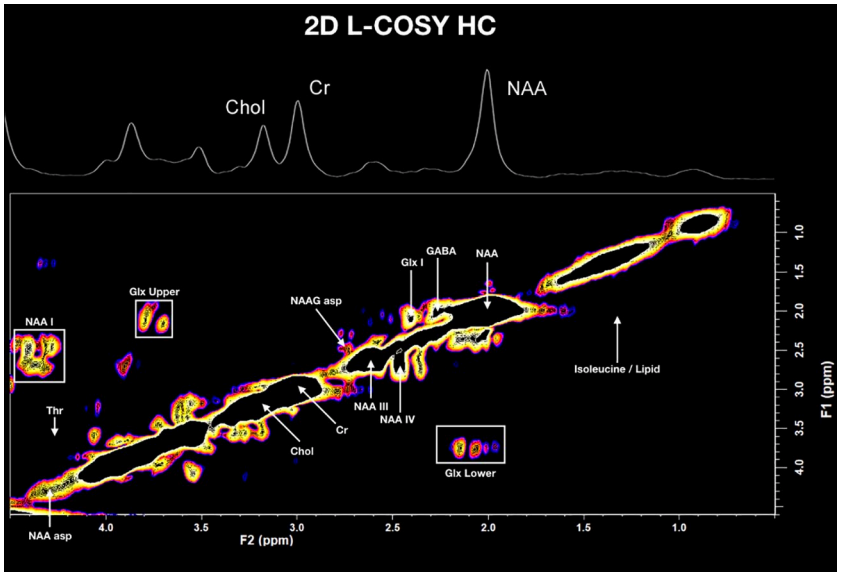

Figure 3. *In vivo* L-COSY of a HC participant (PCC) acquired at 3T, using a 64 channel head and neck coil; voxel size $30 \times 30 \times 30\,mm^3$, increment size 0.8 ms, increments 96, eight averages per increment, TR 1.5 sec, total experimental time 19 min, acquired vector: 1024 points, acquisition time: 512 ms, spectral width in F2: 2000 Hz, spectral width F1: 1250 Hz.
Cr, Creatine; Chol, Choline; GABA, gamma-aminobutyric acid; Glx, glutamine and glutamate cross peaks; HC, healthy control; L-COSY, localized correlation spectroscopy; NAA, N-acetylaspartate; NAA-I, III and IV, additional N-acetylaspartate signatures; NAA asp, NAA aspartate moiety; NAAG, N-acetylaspartylglutamate; PCC, posterior cingulate cortex; Thr, Threonine.

Table 2. Metabolite ratios that significantly differ in the posterior cingulate cortex between healthy subjects and RRMS using 2D L-COSY.

Metabolite	Average chemical shift (F2–F1) ppm	HC	RRMS	% change	*p*-value
NAA	2.00–2.01	135.0 ± 1.1	129.0 ± 1.1	−5%	<0.0001*, **
NAA-I	4.36–2.55	20.3 ± 0.3	18.7 ± 0.3	−8%	<0.0001*, **
NAA-III	2.62–2.62	32.0 ± 0.4	29.9 ± 0.4	−8%	0.002*
NAA-IV	2.47–2.67	8.1 ± 0.1	7.7 ± 0.1	−6%	0.002*
NAA_{amide}	7.81–7.81	1.0 ± 0.1	0.9 ± 0.03	−17%	0.027*
$NAA_{aspartate\ moiety}$	4.30–4.30	5.7 ± 0.1	5.4 ± 0.4	−5%	0.001*
$NAAG_{aspartyl\ moiety}$	2.76–2.47	1.8 ± 0.05	1.6 ± 0.04	−9%	0.027 *
NAA sum	–	204.5 ± 1.6	193.9 ± 1.6	−6%	<0.0001*, **
Threonine	4.27–3.62	1.3 ± 0.1	1.2 ± 0.04	−11%	0.062*
GABA	2.27–1.98	5.7 ± 0.1	5.4 ± 0.1	−5%	0.002*
Glx-I	2.40–2.09	4.9 ± 0.1	4.7 ± 0.1	−6%	0.005*
Glx sum	–	18.1 ± 0.2	17.4 ± 0.2	−4%	0.015*
Glx upper	3.76–2.09	9.2 ± 0.1	8.8 ± 0.1	−4%	0.038
Glx lower	2.10–3.75	8.9 ± 0.1	8.5 ± 0.1	−5%	0.037*
Total Lipids	–	93.4 ± 3.2	113.6 ± 9.3	18%	0.054
Isoleucine/Lipid	1.39–1.95	1.4 ± 0.1	1.2 ± 0.1	−16%	0.028*

GABA, gamma-aminobutyric acid; Glx, glutamine and glutamate cross peaks; Glx sum, contains the above and below the diagonal cross peaks summed; HC, healthy control; L-COSY, localized correlation spectroscopy; NAA, N-acetylaspartate; NAA-I to IV, additional N-acetylaspartate signatures; NAAG, N-acetylaspartylglutamate; NAA sum, sum of NAA cross-peaks; RRMS, relapsing-remitting multiple sclerosis.
All data are expressed as mean metabolite ratio relative to the tCr peak volume ± standard error of the mean unless otherwise indicated.
*Indicates significance (p-value ⩽ 0.05) using Mann–Whitney U tests.
**Indicates significance (p-value ⩽ 0.0007) after Bonferroni Correction.

There was a (−3%) statistically significant reduction in whole brain volume (WBV) in RRMS compared with HC (Table 3). The RMMS group had increased ventricular volume (28%), in keeping with atrophic change and a reduction in WM volume (−5%) when compared with HCs; however, these differences were significant only with parametric (t test) means testing. There was no significant difference in the total or peripheral grey matter volumes (GMV). On average, RRMS participants had a total T2 FLAIR lesion volume of 6.7 ml.

Correlation of metabolites with clinical and volumetric measures

Multiple correlations between the NAA chemical fingerprints, clinical, and demographic measures were identified (Table 4). Specifically, NAA-I showed a strong negative correlation, and NAA-III and Glx-I showed a moderately negative correlation with disease duration. As expected, NAA signatures were negatively correlated with age. Macromolecules were the only species correlated with disease severity (MSSS and EDSS); however, this should be interpreted with caution as no significant group difference was identified.

Table 3. Comparison of whole brain volumes and partial volumes within the MRS voxel.

Volumetric measure	HC ($n=40$)	RRMS ($n=45$)	Difference (%)	p-value
Voxel CSF (%)	11.89 ± 0.79	12.62 ± 0.75	6%	0.64
Voxel GM (%)	50.91 ± 0.46	50.46 ± 0.57	−1%	0.11
Voxel WM (%)	36.82 ± 0.75	36.92 ± 0.61	0%	0.67
WBV (mL)	1617.5 ± 13.7	1572.5 ± 14.3	−3%	0.03*
WM (mL)	790.9 ± 7.0	756.1 ± 6.7	−5%	0.001
GM (mL)	826.6 ± 8.7	816.4 ± 9.1	−1%	0.4
cGM (mL)	665.7 ± 7.4	658.2 ± 7.4	−1%	0.5
CSF (mL)	29.6 ± 1.2	41.2 ± 2.8	28%	0.001
Mean lesion volume (mL)	n/a	6.7	n/a	n/a

cGM, normalised cortical grey matter; CSF, normalised cerebrospinal fluid volume; GM, normalised grey matter volume; HC, healthy control; MRS, magnetic resonance spectroscopy; RRMS, relapsing-remitting multiple sclerosis; WBV, normalised whole brain volume; WM, normalised white matter volume.
*Indicates significance (p-value < 0.05) using Mann–Whitney U tests.

Multiple correlations between molecular species and cognitive function were identified. Cognitive assessment (total ARCS) was negatively correlated with summed Glx cross peaks, and the isoleucine/lipid cross peak (Pearson's correlation: −0.30 and −0.39, p-value = 0.046 and 0.008, respectively). Visuospatial cognitive function was negatively correlated with NAA-I, Glx-I (shown in Figure 4) and the NAAG aspartate moiety cross peak (Pearson's correlation: −0.41, −0.39, and −0.33, p-values = 0.005, 0.007, and 0.025, respectively). Attention was moderately negatively correlated with the isoleucine/lipid cross peak (Pearson's correlation: −0.39, p-value = 0.004), as shown in Figure 4.

NAA signatures were significantly positively correlated with WBV, but also with GMV, and white matter volume (WMV) individually. CSF volume was moderately negatively correlated with NAA signatures. The Glx-I cross peak was moderately positively correlated with GM volume. Subcortical GMVs were positively correlated with the same NAA signatures, which were significantly correlated with total GMV. A single cross peak, tentatively assigned to isoleucine/lipid, was significantly and positively correlated with total lesion number, but not with lesion volume.

No correlations retained significance when correction for multiple comparisons was applied.

Correlation between clinical and volumetric measures

Of the brain volume measurements, GMV and total lesion volume (TLV) were the most closely associated with cognitive function and disease severity. None of the volumetric parameters tested predicted fatigue, and only the combined score of depression, anxiety, and stress correlated weakly with WMV. TLV was strongly negatively correlated with WBV and GMV (Pearson's correlation: −0.64 and −0.59, $p \leq 0.001$ for both).

No correlations retained significance when corrected for multiple comparisons.

Discussion

Our RRMS patient cohort was comprised of patients who were clinically stable and currently undergoing treatment with Fingolimod. The lesion load was low in these patients and current disability status was mild, at an EDSS value of 2. The MRS voxel, located in the PCC and evaluated by 2D L-COSY, predominantly contained normal appearing WM and GM. Whilst disability status was mild, there was evidence of impaired cognitive function and higher levels of mood and fatigue symptoms in RRMS compared with matched healthy subjects. Despite a stable

Table 4. Significant correlations between 2D L-COSY metabolite levels in the posterior cingulate cortex, whole brain volumes and lesion load of RRMS patients *versus* clinical symptoms and brain volumes.

Clinical measure	Metabolite	Correlation	*p*-value
Age	NAA-I	−0.52	<0.001*
	NAA sum	−0.43	<0.001*
	Glx-I	−0.41	<0.005*
	cGM	−0.49	<0.001*
MS disease duration	NAA-III	−0.54	<0.001*
	NAA-I	−0.32	<0.03*
	Glx-I	−0.40	0.006*
	WBV	−0.48	<0.001*
	CSF	−0.50	<0.001*
MSSS	Macromolecules	0.42	0.004*
EDSS	Macromolecules	0.31	0.04*
	cGM	−0.49	<0.001*
	TLV	0.46	0.001*
DASS	WM	0.34	0.02
Cognitive Function			
ARCS	Total Glx	−0.30	0.046*
	Isoleucine/Lipid	−0.39	0.008*
	TLV	−0.33	0.03
Visuospatial	NAA-I	−0.41	0.005*
	Glx-I	−0.39	0.0074*
	$NAAG_{aspartate}$	−0.33	0.025*
Attention	Isoleucine/Lipid	−0.39	0.004*
	TLV	−0.41	0.005
Memory	Isoleucine/Lipid	−0.44	0.002*
Fluency	WM	0.31	0.04
	TLV	−0.35	0.02
SDMT	WBV	0.34	0.02
	GM	0.34	0.02
	cGM	0.39	0.008
	TLV	−0.4	0.006

(Continued)

Table 4. (Continued)

Clinical measure	Metabolite	Correlation	*p*-value
Whole brain volumes and lesion load			
WBV	NAA	0.4	0.006*
	NAA sum	0.43	0.003*
	TLV	−0.64	<0.001*
GM	NAA	0.40	0.006*
	NAA-III	0.45	0.002*
	NAA-IV	0.40	0.007*
	NAA sum	0.46	0.002*
	Glx-I	0.36	0.02*
	TLV	−0.59	<0.001*
WM	NAA	0.31	0.04*
	TLV	−0.37	0.013
CSF	NAA-III	−0.37	0.013*
	NAA sum	−0.30	0.048*
	TLV	0.38	0.001
TLN	Isoleucine/Lipid	0.44	0.003*

ARCS, Audio Recorded Cognitive Screen; cGM, Cortical Grey Matter; CSF, Cerebrospinal Fluid Volume; DASS, Depression Anxiety and Stress Scale; EDSS, Expanded Disability Status Scale; GABA, gamma-aminobutyric acid; Glx, glutamine and glutamate cross peaks; GM, Grey Matter volume; L-COSY, localized correlation spectroscopy; MSSS, Multiple Sclerosis Severity Scale; NAA, N-acetylaspartate; NAA-I to IV, additional N-acetylaspartate signatures; NAAG, N-acetylaspartylglutamate; NAA sum, sum of NAA cross-peaks; SDMT, Symbol Digit Modalities Test; TLN, Total Lesion Number; TLV, Total Lesion volume; WBV, normalised whole brain volume; WM, White Matter volume.
Correlations are made between 2D L-COSY metabolite levels and demographics, clinical symptoms and partial brain volumes in the RRMS ($n = 45$) group.
Pearson's correlations are shown.
*Indicates significance (p-value $\leqslant 0.05$) using Spearman's test.

disease status, we were able to detect metabolic alterations in the MS brain in NABM, which were comparable to those observed in other studies.[4,32–35] These differences cannot be attributed to morphological differences in the region of interest between control and MS patients, as there were no differences in the WM, GM, or CSF MRS voxel composition between groups. The lack of a strong association between whole brain lesion volume and the presence of clinical symptoms in our cohort highlights the clinico-radiological paradox, and supports a potential use of MRS to identify other contributing pathological factors in MS.

Using 2D L-COSY, we identified a reduction in multiple NAA metabolic fingerprints, and the summed glutamine and glutamate metabolic signatures. 2D L-COSY also enabled the identification of additional metabolic MS-specific changes, not quantifiable using other techniques, such as GABA, that historically requires an edited pulse sequence for accurate quantification.[36]

A reduction in NAA has been shown by others as the most consistent metabolic abnormality found in NABM in the MS brain.[37] The metabolic fingerprints of NAA in the PCC were significantly correlated with reductions in all whole brain

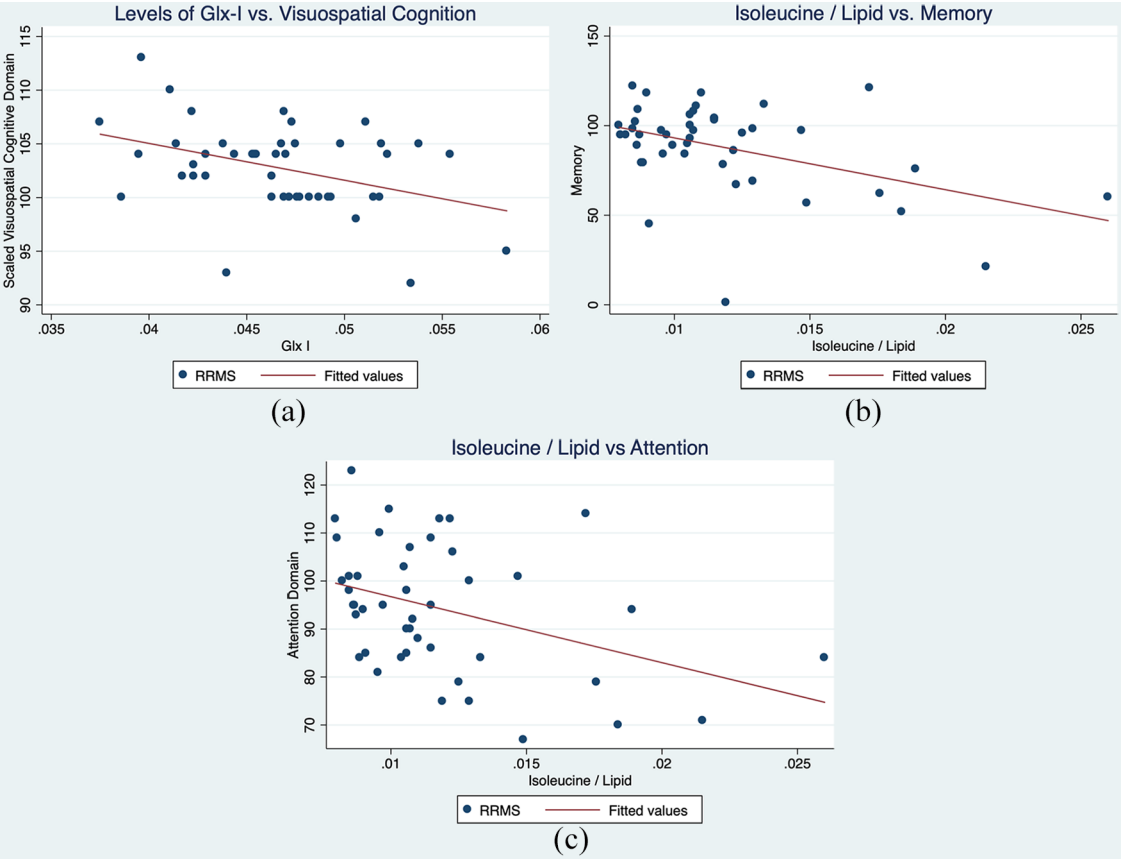

Figure 4. Scatter plots showing the relationship between (a) Glx-I *versus* visuospatial cognition, isoleucine/lipid *versus* memory; and (b) isoleucine/lipid *versus* attention.
Glx, glutamate.

volumetric measures, with a strong correlation with WBV. A statistically significant reduction in the WBV was identified in the RRMS group (−3%); however, we were able to detect a greater reduction in NAA fingerprints (NAA sum: −6% and up to −17% for the NAA amide moiety) in the normal-appearing PCC of the MS group. These findings suggest that NAA may be a more sensitive marker of parenchymal volume loss when compared with volumetric measures. NAA levels were also associated with disease duration, which may also be linked with increased brain atrophy during the course of the disease.[38] Longitudinal studies are required to further clarify this finding and to determine if techniques such as whole brain NAA can further increase the sensitivity and clinical usefulness of MRS.[39]

We identified a small, but statistically significant, reduction in Glx in NABM that was negatively associated with cognitive function (total ARCS), specifically in the visuospatial domain. Additionally, Glx was negatively correlated with disease duration. This finding supports the work of Muhlert and colleagues, who identified reductions in glutamate in the cingulate and parietal cortices, associated with reduced visuospatial memory in MS patients.[33] One possible explanation for this finding is reduced synaptic activity due to synaptic loss,[40] which is also supported by findings in the ageing brain.[41] This is further supported by the significant positive correlation that was identified between a single Glx cross peak (Glx-I) and whole brain GM volume.

GABA is the major inhibitory neurotransmitter in the brain. Our results of decreasing GABA in PCC agree with recent RRMS work performed by Cao and colleagues, where they detected a decrease in GABA+, which has contributions from MM and homocarnosine.[42] Additionally, another study found reduced GABA levels in secondary

progressive patients in the hippocampus and the sensorimotor cortex, associated with reduced motor performance.[17] This decrease in GABA may be due to a decline of GABAergic neurons and related enzymes.[43] In the current study, we did not find a correlation between GABA, brain volume, or cognitive function, most likely due to the early disease stage of our cohort.

Isoleucine is an essential amino acid. This is the first *in vivo* evidence of a reduction of isoleucine in the brain in MS. Supporting this finding, Hyun-Hwi and colleagues found reduced isoleucine in the CSF of patients with MS who were in relapse, when compared with patients in remission, using *in vitro* MRS.[44] Isoleucine was associated with multiple measures of cognitive function, including total ARCS, attention, and memory domains of cognitive function. Further work is required to confirm these findings, as the cross peak for isoleucine is in a location where there is contamination from T1 noise and lipid.

A second amino acid, threonine, was found to be significantly reduced between RRMS patients and HCs. Threonine was not correlated with clinical symptoms or volume measures. Mader and colleagues have described a possible elevation in alanine, threonine, valine, leucine, and isoleucine, using metabolite nulled MRS in acute MS lesions.[45] They hypothesized that, because these amino acids have been shown to be contained within myelin, that the increase may be secondary to cleavage of myelin proteins, which could be a result of oligodendrocyte pathology.[45] As far as we are aware, this is the first study to show a reduction of the amino acids contained within myelin in NABM.

Despite a low whole brain lesion load, we did observe an overall −3% reduction in total brain volume and −5% loss in WM content, with a reciprocal 28% increase in CSF content, compared with healthy age and sex-matched controls. Lower brain volumes have been linked to an increased risk of disease progression rates, and reduced the effect of therapy in MS cases,[46] supporting the notion that disease processes other than WM demyelination are occurring in the MS brain. The rate of atrophy continues to be investigated as a potential marker of disease progression in MS,[47] and, indeed, regional atrophy in GM structures, particularly the thalamus, have been shown to have a high correlation of cognitive performance in MS.[48] Although the current study was cross-sectional, from which we cannot evaluate the time-dependent level of atrophy, we do see a moderate positive association between WBV, cortical GM, and GMV with cognitive function as determined by the SDMT (Table 4).

Currently, 2D L-COSY technology has some limitations, such as the high SNR requirement for adequate data quality, thus the time of acquisition is currently 19 min. Work is currently being undertaken by our group and others to accelerate 2D L-COSY.[49] Like with many SVS techniques, the 2D L-COSY voxel needs to be large (~27 cm^3), limiting the accuracy with which brain regions can be interrogated.

This study has been carried out with a small number of participants (total $n = 45$ per group). Despite this, every effort has been made to control for confounding variables by age and sex-matching the groups. Ongoing investigations are warranted, to undertake longitudinal evaluations of changes in metabolites to further appreciate the biochemical processes that underpin the changes in metabolite levels we observed, and assess the usefulness of these chemical entities as potential biomarkers for disease severity and progression. Treatment response was not an endpoint in our current study, as the focus was on stable patients. Further work is needed to determine how the metabolites identified in this study are related to treatment.

Conclusion

Using 2D L-COSY, we were able to report on metabolites that were otherwise not available for analysis using 1D spectroscopy. Using 2D L-COSY, we provide *in vivo* evidence of a reduction in multiple NAA signatures, GABA, Glx, and isoleucine/lipid in NABM of RRMS patients correlating with clinical outcome. The additional metabolic information provided may be helpful in the future to unlock the pathophysiology of RRMS and identifying biomarkers for RRMS, disease severity, and clinical progression.

Acknowledgments

We would like to acknowledge all the study participants that took part in this investigation.

Funding

The authors disclosed receipt of the following financial support for the research, authorship,

and publication of this article: Funding for this study provided by Novartis Pharmaceuticals Australia.

Conflict of interest statement

The authors declare that there is no conflict of interest.

ORCID iD

Scott Quadrelli https://orcid.org/0000-0002-6626-9825

References

1. Barkhof F. The clinico-radiological paradox in multiple sclerosis revisited. *Curr Opin Neurol* 2002; 15: 239–245.
2. Chard D and Trip SA. Resolving the clinico-radiological paradox in multiple sclerosis. *F1000Res* 2017; 6: 1828.
3. Healy BC, Buckle GJ, Ali EN, *et al.* Characterizing clinical and MRI dissociation in patients with multiple sclerosis. *J Neuroimaging* 2017; 27: 481–485.
4. Geurts JJ, Reuling IE, Vrenken H, *et al.* MR spectroscopic evidence for thalamic and hippocampal, but not cortical, damage in multiple sclerosis. *Magn Reson Med* 2006; 55: 478–483.
5. Bermel RA and Bakshi R. The measurement and clinical relevance of brain atrophy in multiple sclerosis. *Lancet Neurol* 2006; 5: 158–170.
6. Roosendaal SD, Bendfeldt K, Vrenken H, *et al.* Grey matter volume in a large cohort of MS patients: relation to MRI parameters and disability. *Mult Scler* 2011; 17: 1098–1106.
7. Miller DH, Lublin FD, Sormani MP, *et al.* Brain atrophy and disability worsening in primary progressive multiple sclerosis: insights from the informs study. *Ann Clin Transl Neurol* 2018; 5: 346–356.
8. Shiee N, Bazin PL, Zackowski KM, *et al.* Revisiting brain atrophy and its relationship to disability in multiple sclerosis. *PLoS One* 2012; 7: e37049.
9. Narayana PA. Magnetic resonance spectroscopy in the monitoring of multiple sclerosis. *J Neuroimaging* 2005; 15: 46S–57S.
10. Londono AC and Mora CA. Nonconventional MRI biomarkers for in vivo monitoring of pathogenesis in multiple sclerosis. *Neurol Neuroimmunol Neuroinflamm* 2014; 1: e45.
11. Fleischer V, Kolb R, Groppa S, *et al.* Metabolic patterns in chronic multiple sclerosis lesions and normal-appearing white matter: intraindividual comparison by using 2d MR spectroscopic imaging. *Radiology* 2016; 281: 536–543.
12. Steen C, D'haeseleer M, Hoogduin JM, *et al.* Cerebral white matter blood flow and energy metabolism in multiple sclerosis. *Mult Scler* 2013; 19: 1282–1289.
13. Khan O, Seraji-Bozorgzad N, Bao F, *et al.* The relationship between brain MR spectroscopy and disability in multiple sclerosis: 20-year data from the U.S. Glatiramer Acetate extension study. *J Neuroimaging* 2017; 27: 97–106.
14. Aboul-Enein F, Krssak M, Hoftberger R, *et al.* Reduced NAA-levels in the NAWM of patients with MS is a feature of progression. A study with quantitative magnetic resonance spectroscopy at 3 Tesla. *PLoS One* 2010; 5: e11625.
15. Obert D, Helms G, Sattler MB, *et al.* Brain metabolite changes in patients with relapsing-remitting and secondary progressive multiple sclerosis: a two-year follow-up study. *PLoS One* 2016; 11: e0162583.
16. Yetkin MF, Mirza M and Donmez H. Monitoring interferon beta treatment response with magnetic resonance spectroscopy in relapsing remitting multiple sclerosis. *Medicine (Baltimore)* 2016; 95: e4782.
17. Cawley N, Solanky BS, Muhlert N, *et al.* Reduced gamma-aminobutyric acid concentration is associated with physical disability in progressive multiple sclerosis. *Brain* 2015; 138: 2584–2595.
18. Keeler J. *Understanding NMR spectroscopy*. 2nd ed. Chichester: John Wiley and Sons, 2010.
19. Mountford C, Quadrelli S, Lin A, *et al.* Six fucose-alpha(1-2) sugars and alpha-fucose assigned in the human brain using in vivo two-dimensional MRS. *NMR Biomed* 2015; 28: 291–296.
20. Ramadan S, Ratai EM, Wald LL, *et al.* In vivo 1D and 2D correlation MR spectroscopy of the soleus muscle at 7T. *J Magn Reson* 2010; 204: 91–98.
21. Thomas MA, Yue K, Binesh N, *et al.* Localized two-dimensional shift correlated MR spectroscopy of human brain. *Magn Reson Med* 2001; 46: 58–67.
22. Arm J, Al-Iedani O, Quadrelli S, *et al.* Reliability of neurometabolite detection with two-dimensional localized correlation spectroscopy at 3T. *J Magn Reson Imaging* 2018; 48: 1559–1569.

23. Kurtzke JF. Rating neurologic impairment in multiple sclerosis: an expanded disability status scale (EDSS). *Neurology* 1983; 33: 1444–1452.

24. Roxburgh RH, Seaman SR, Masterman T, *et al.* Multiple sclerosis severity score: using disability and disease duration to rate disease severity. *Neurology* 2005; 64: 1144–1151.

25. Leech R and Sharp DJ. The role of the posterior cingulate cortex in cognition and disease. *Brain* 2014; 137: 12–32.

26. Arm J, Al-iedani O, Lea R, *et al.* Diurnal variability of cerebral metabolites in healthy human brain with 2D localized correlation spectroscopy (2D L-COSY). *J. Magn. Reson. Imaging* 2019; 50: 592–601. doi:10.1002/jmri.26642

27. Mathworks. Matlab, 7.0.1.24704 (R14) ed. 1984–2014.

28. Accelrys Felix Nmr. Felix Nmr, 2007 ed.

29. Schmidt P, Gaser C, Arsic M, *et al.* An automated tool for detection of flair-hyperintense white-matter lesions in multiple sclerosis. *Neuroimage* 2012; 59: 3774–3783.

30. Smith SM, Zhang Y, Jenkinson M, *et al.* Accurate, robust, and automated longitudinal and cross-sectional brain change analysis. *Neuroimage* 2002; 17: 479–489.

31. Smith SM, Jenkinson M, Woolrich MW, *et al.* Advances in functional and structural MR image analysis and implementation as FSL. *Neuroimage* 2004; 23(Suppl. 1): S208–S219.

32. Kapeller P, Mclean MA, Griffin CM, *et al.* Preliminary evidence for neuronal damage in cortical grey matter and normal appearing white matter in short duration relapsing-remitting multiple sclerosis: a quantitative MR spectroscopic imaging study. *J Neurol* 2001; 248: 131–138.

33. Muhlert N, Atzori M, De Vita E, *et al.* Memory in multiple sclerosis is linked to glutamate concentration in grey matter regions. *J Neurol Neurosurg Psychiatry* 2014; 85: 833–839.

34. Richards TL. Proton MR spectroscopy in multiple sclerosis: value in establishing diagnosis, monitoring progression, and evaluating therapy. *AJR Am J Roentgenol* 1991; 157: 1073–1078.

35. Tisell A, Leinhard OD, Warntjes JB, *et al.* Increased concentrations of glutamate and glutamine in normal-appearing white matter of patients with multiple sclerosis and normal MR imaging brain scans. *PLoS One* 2013; 8: e61817.

36. Mescher M, Merkle H, Kirsch J, *et al.* Simultaneous in vivo spectral editing and water suppression. *NMR Biomed* 1998; 11: 266–272.

37. Rovira A and Alonso J. 1H magnetic resonance spectroscopy in multiple sclerosis and related disorders. *Neuroimaging Clin N Am* 23: 459–474.

38. Eshaghi A, Marinescu RV, Young AL, *et al.* Progression of regional grey matter atrophy in multiple sclerosis. *Brain* 2018; 141: 1665–1677.

39. Gonen O, Catalaa I, Babb JS, *et al.* Total brain N-acetylaspartate: a new measure of disease load in Ms. *Neurology* 2000; 54: 15–19.

40. Wegner C, Esiri MM, Chance SA, *et al.* Neocortical neuronal, synaptic, and glial loss in multiple sclerosis. *Neurology* 2006; 67: 960–967.

41. Kaiser LG, Schuff N, Cashdollar N, *et al.* Age-related glutamate and glutamine concentration changes in normal human brain: 1H MR spectroscopy study at 4 T. *Neurobiol Aging* 2005; 26: 665–672.

42. Cao G, Edden RaE, Gao F, *et al.* Reduced GABA levels correlate with cognitive impairment in patients with relapsing-remitting multiple sclerosis. *Eur Radiol* 2018; 28: 1140–1148.

43. Dutta R, McDonough J, Yin X, *et al.* Mitochondrial dysfunction as a cause of axonal degeneration in multiple sclerosis patients. *Ann Neurol* 2006; 59: 478–489.

44. Kim HH, Jeong IH, Hyun JS, *et al.* Metabolomic profiling of CSF in multiple sclerosis and neuromyelitis optica spectrum disorder by nuclear magnetic resonance. *PLoS One* 2017; 12: e0181758.

45. Mader I, Seeger U, Weissert R, *et al.* Proton MR spectroscopy with metabolite-nulling reveals elevated macromolecules in acute multiple sclerosis. *Brain* 2001; 124: 953–961.

46. Sormani MP, Kappos L, Radue EW, *et al.* Defining brain volume cutoffs to identify clinically relevant atrophy in RRMS. *Mult Scler* 2017; 23: 656–664.

47. De Stefano N, Stromillo ML, Giorgio A, *et al.* Establishing pathological cut-offs of brain atrophy rates in multiple sclerosis. *J Neurol Neurosurg Psychiatry* 2016; 87: 93–99.

48. Bergsland N, Zivadinov R, Dwyer MG, *et al.* Localized atrophy of the thalamus and slowed cognitive processing speed in MS patients. *Mult Scler* 2016; 22: 1327–1336.

49. Verma G, Chawla S, Nagarajan R, *et al.* Non-uniformly weighted sampling for faster localized two-dimensional correlated spectroscopy of the brain in vivo. *J Magn Reson* 2017; 277: 104–112.
50. Ramadan S, Andronesi OC, Stanwell P, *et al.* Use of in vivo two-dimensional MR spectroscopy to compare the biochemistry of the human brain to that of glioblastoma. *Radiology* 2011; 259: 540–549.
51. Gelineau-Morel R, Tomassini V, Jenkinson M, *et al.* The effect of hypointense white matter lesions on automated gray matter segmentation in multiple sclerosis. *Hum Brain Mapp* 2012; 33: 2802–2814.
52. Battaglini M, Jenkinson M and De Stefano N. Evaluating and reducing the impact of white matter lesions on brain volume measurements. *Hum Brain Mapp* 2012; 33: 2062–2071.
53. Zhang Y, Brady M and Smith S. Segmentation of brain MR images through a hidden Markov random field model and the expectation-maximization algorithm. *IEEE Trans Med Imaging* 2001; 20: 45–57.
54. Quadrelli S, Mountford C and Ramadan S. Hitchhiker's guide to voxel segmentation for partial volume correction of in vivo magnetic resonance spectroscopy. *Magn Reson Insights* 2016; 9: 1–8.
55. Smith SM. Fast robust automated brain extraction. *Hum Brain Mapp* 2002; 17: 143–155.
56. Jenkinson M and Smith S. A global optimisation method for robust affine registration of brain images. *Med Image Anal* 2001; 5: 143–156.
57. Jenkinson M, Bannister P, Brady M, *et al.* Improved optimization for the robust and accurate linear registration and motion correction of brain images. *NeuroImage* 2002; 17: 825–841.

Appendix 1

Additional methods

Clinical assessments. Study participants were assessed for cognitive performance using the Audio Recorded Cognitive Screen (ARCS), which is a valid and reliable instrument for administering neuropsychological tests of cognitive function to unsupervised individuals. The ARCS assesses performance in the domains of memory, verbal fluency, language (object naming), visuospatial function, and attention, with elements from each domain score then used to derive an overall 'global' cognitive performance score. A lower score in these cognitive domains indicates a poorer performance. The Symbol Digit Modalities Test (SDMT) was undertaken concurrently as a measure of attention and information processing speed presented in the visual modality, a lower score indicating reduced processing speed.

Participants own rating of cognitive functioning was assessed using the Functional Assessment Questionnaire (FAQ), where higher values indicate poorer self-reported cognitive function.

The mental health status of participants was assessed using the short version of the Depression Anxiety Stress Scales (DASS-21). Higher scores were indicative of higher levels of depression, stress and anxiety. All scores, derived from the 21-point scale, were multiplied by 2 to enable comparison to the full 42-point scale DASS and determine clinical cutoffs for symptom severity.

Fatigue status was determined using the Modified Fatigue Impact Scale (MFIS), a modified form of the Fatigue Impact Scale. The questionnaire was based on items derived from interviews with MS patients concerning how fatigue impacts their lives. This instrument provided an assessment of the effects of fatigue in terms of physical and cognitive functioning, as well as 'total fatigue', higher scores indicate greater levels of fatigue.

2D L-COSY acquisition parameters. RF carrier frequency at 2.0 ppm; TR 1.5 s; water suppression using WET; 96 t1 increments; with eight averages per increment; PCC voxel size $3 \times 3 \times 3\,cm^3$, acquired vector size 1024 points; acquisition time 512 ms; spectral width in F2 2000 Hz and spectral width in F1 1250 Hz (0.8 ms increment size), total acquisition time of 19 min. Additional details can be found in Ramadan and colleagues.[50]

Localized shimming was undertaken by adjustment of zero- and first-order shim gradients using the automatic B0 field mapping technique supplied by the vendor (Siemens AG, Erlangen, Germany) followed by manual adjustment of accessible shim gradients to achieve a resulting magnitude peak width of water at half-maximum of 15 Hz or less.

WM lesion quantification. The lesion growth algorithm[29] as implemented in the LST toolbox (version 2.0.6) first segments the T1 images into the

three main tissue classes: CSF, GM, and WM. This information is then combined with the coregistered FLAIR intensities in order to calculate lesion belief maps. By thresholding these maps with a prechosen initial threshold (κ), an initial binary lesion map was obtained, which was subsequently grown along voxels that appear hyperintense in the FLAIR image, resulting in a lesion probability map. The initial κ threshold was selected by iterating κ and performing a visual inspection, for this data set a κ value of 0.1 was selected. A binary lesion mask was created for each participant using a threshold of 0.5. Hypointense lesions on the T1 MPRAGE were determined using the binary lesion mask and filled with intensities similar to voxels not contained within a lesion (referred to as 'lesion filling'), using the LST toolbox.[29] Lesion filling was performed to improve volume measurements and prevent errors in partial volume segmentation.[51,52] Partial volume segmentation of the lesion filled T1 structural image was segmented using FSL FAST[53] after brain extraction. The values obtained from FSL FAST were used to determine the parenchymal partial volumes contained within the SVS voxel as described by Quadrelli and colleagues.[54]

Brain volume quantification. SIENAX extracts brain and skull images from the single whole-head input data.[55] The brain image was then affine-registered to MNI152 space (using the skull image to determine the registration scaling)[56,57]; this was done to obtain the volumetric scaling factor, then used as normalization for head size. Next, tissue-type segmentation with partial volume estimation was carried out in order to calculate the total volume of brain tissue, including separate estimates of volumes of GM, WM, peripheral GM, and ventricular CSF.[53]

2D L-COSY quantification. The processing parameters used were: F2 domain (skewed sine-squared window, 2048 points, magnitude mode), F1 domain (sine-squared window, linear prediction to 96 points, zero-filling to 512 points, magnitude mode). No additional water removal was applied, as water was sufficiently suppressed during acquisition. The volumes of cross peaks, or diagonal resonances, were evaluated using Felix software described above, and care was taken to ensure that the interrogated volume was the same in all 2D spectra, using a peak template with fixed chemical shift values.